Gorge 2nd Tunnel

Preliminary Geotechnical Data Report

January 21, 2010

Seattle City Light

Prepared by:

Aspect Consulting, LLC
401 Second Avenue S, Suite 201
Seattle, WA 98104

Jacobs Associates
1109 First Avenue Suite 501
Seattle, WA 98101

Distribution

To: John Owen, PE
Seattle City Light

Dave Rowan, PE
Seattle City Light

From: Gregg Davidson, PE
Jacobs Associates

Prepared By: Annaliese Eipert
Aspect Consulting

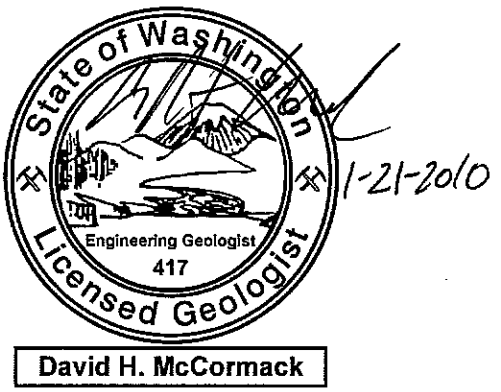

Dave McCormack, LEG
Aspect Consulting

Susan L. Bednarz, RG
Jacobs Associates

Reviewed By: Gregg Davidson, PE
Jacobs Associates

Mark Havekost, PE
Jacobs Associates

Susan L. Bednarz, RG
Jacobs Associates

Table of Contents

Distribution ii
Table of Contents iii
List of Tables iv
List of Figures iv
List of Appendices iv
1 Introduction 1
1.1 Purpose 1
1.2 Report Organization 1
1.3 Project Datum 1
1.4 Scope 1
2 Site and Project Overview 2
2.1 Project Description and Site History 2
2.2 Geologic Overview of Project Area 2
3 Methodology 4
3.1 Data Review 4
3.2 Field Exploration Program 5
3.3 Laboratory Testing 8
4 Subsurface Observations 10
4.1 Rock Types 10
4.2 Fractures 13
4.3 Surficial Deposits 14
4.4 Drilling Conditions 14
4.5 Groundwater Observations 14
4.6 In Situ Hydraulic Conductivity (Packer) Testing Results 15
5 Reference Data Sources 16
6 References 17
7 Limitations 18

List of Tables

Table 1	Borehole Data Summary
Table 2	Borehole At-Time-of-Drilling (ATD) Groundwater Summary
Table 3	Borehole Flow Summary
Table 4	In Situ Hydraulic Conductivity (Packer) Testing Summary
Table 5	Petrographic Analysis Results Summary
Table 6	Unconfined Compressive Strength (UCS) Results Summary
Table 7	Fracture Density by Borehole
Table 8	Fracture Density by Rock Type

List of Figures

Figure 1	Site Vicinity Map
Figure 2	Project Features and Borehole Locations
Figure 3	Topographic Lineaments on LiDAR Hillshade Image
Figure 4	B-1 Rock Type Distribution Histogram
Figure 5	B-2 Rock Type Distribution Histogram
Figure 6	B-3 Rock Type Distribution Histogram
Figure 7	B-4 Rock Type Distribution Histogram
Figure 8	B-5 Rock Type Distribution Histogram
Figure 9	B-6 Rock Type Distribution Histogram
Figure 10	Unconfined Compressive Strength (UCS) Histogram
Figure 11	Point Load Test Strength Histogram
Figure 12	Fracture Density Histogram
Figure 13	Rock Quality Designation (RQD) Histogram

List of Appendices

APPENDIX A	Borehole Logs
APPENDIX B	Drill Core Photos
APPENDIX C	Laboratory Testing Data
APPENDIX D	Groundwater Data
APPENDIX E	Packer Test Data
APPENDIX F	Feature Orientations
APPENDIX G	Oriented Borehole Images
APPENDIX H	LiDAR Hillshade Images
APPENDIX I	Existing Data

1 Introduction

This Preliminary Geotechnical Data Report (GDR) presents geologic and geotechnical data obtained by Jacobs Associates (JA) and Aspect Consulting, LLC (Aspect) for the Seattle City Light Gorge 2nd Tunnel (G2T) project.

1.1 Purpose

The Preliminary GDR presents a summary of geologic and geotechnical data gathered during the field investigation and laboratory testing phase of the proposed Gorge 2nd Tunnel project. The primary purpose of this data report is to present information that can be used to characterize geologic conditions for the design and construction of the G2T project. Interpretations of this data and its relation to tunnel construction will be presented in a subsequent Geotechnical Baseline Report.

1.2 Report Organization

This report is organized in seven sections. Section 1 provides general introductory information, Section 2 describes the site and project area, Section 3 outlines the methodology used, Section 4 describes subsurface conditions, Section 5 summarizes existing data sources, Section 6 lists references, and Section 7 presents limitations. Figures and summary tables follow the text. All appendices are attached at the end of the report, in hard-copy or as part of a disc. Each appendix includes a summary page listing its contents and the location and format of each item.

1.3 Project Datum

All elevations within this report are referenced to vertical datum NAVD88. Locations are referenced to horizontal datum NAD83-98 Washington State Plane.

1.4 Scope

This report presents data gathered during field investigation and laboratory testing programs for the G2T tunnel design and construction project. This report is not intended to provide interpretation of the data.

2 Site and Project Overview

2.1 Project Description and Site History

The Gorge Powerhouse facilities are located on the Skagit River near Newhalem, Washington, about 90 miles northeast of Seattle (Figure 1). The Gorge Powerhouse and existing 11,000-foot long, 20.5-foot internal diameter, concrete-lined tunnel (G1T) were built by the Seattle City Light (SCL) public utility following approval of hydroelectric facilities on the Skagit River by the federal government in 1918. The facilities at Gorge Dam began providing power to Seattle in 1924. The original tunnel, still in service to this day, initially conveyed water to three turbine units. In 1949, SCL was authorized to expand the Powerhouse, build the Gorge High Dam, and install an additional powerhouse and generator. These additions increased overall power output but the faster-moving water increased friction along the tunnel walls, thereby reducing the available head and decreasing efficiency of the turbines.

For nearly 20 years, SCL has been considering a second parallel power tunnel as a way to optimize the existing Gorge Powerhouse facilities. The Gorge 2nd Tunnel is anticipated to be a largely unlined, 20- to 22-foot-diameter tunnel bored between the Gorge Powerhouse and the intake at Gorge Dam (Figure 2). It will parallel the existing tunnel and will increase generating efficiency by reducing head loss. This will allow SCL to better optimize power generation without exceeding flow limits into the Skagit River, a fisheries management requirement.

2.2 Geologic Overview of Project Area

2.2.1 General Geology

The project area is located in the North Cascades range of north-central Washington State. The North Cascades is a tectonically complex series of geologic terranes that have accreted over the last 400 million years to form the landmass of western North America. Newhalem and the Gorge Power Station are located in the metamorphic core of the North Cascades, the zone of deformation between two major fault zones that has been uplifted approximately 7 to 11 miles relative to the rocks on either side (Tabor *et al*., 2003). The bedrock at the project site has been thoroughly metamorphosed and exposed to various episodes of igneous intrusions, and faulting and shearing, which have created zones of weakness that must be considered throughout the development of the project.

2.2.2 Geomorphology

The Gorge Powerhouse facilities are located in the glacially carved Skagit River valley. The area's geomorphology is largely defined by steep bedrock valleys that were modified by glaciers during the most recent ice ages. Glacial sediments were also deposited and are still preserved in some areas. Rivers and seasonal drainages carrying water westward from the crest of the Cascade Mountains slowly erode into the bedrock, but have modified the landscape only slightly since the last glaciation.

The squeezing, faulting, and folding of the bedrock during millennia of tectonic activity has also contributed to the area's geomorphology, as is reflected in some of the more linear drainages, where flowing water has exploited the weakened rocks within fault zones. Rockfall is common in weakened fault zones and elsewhere in the project area, and has built talus slopes along the base of the Skagit River

valley and on other slopes. Winter snow avalanches can also carry and deposit rocks, debris and vegetation downslope.

2.2.3 Bedrock

Bedrock along the tunnel alignment consists primarily of orthogneiss, a foliated (mineralogically-banded), metamorphosed igneous rock. Specifically, the orthogneiss in the alignment area is a member of the Middle Eocene to Late Cretaceous-age Skagit Gneiss Complex of the North Cascades, which crops out mostly between Newhalem and Ross Lake, to the east. Concordant (parallel to bedrock strata) and discordant (cutting across bedrock strata) intrusions of igneous rocks are present within the metamorphic bedrock. Project area bedrock is discussed in more detail in Section 4 of this report.

2.2.4 Structures

Secondary geologic structures are formed in bedrock due to regional tectonic and other localized stresses on the rock following their original emplacement/deposition. Structures include: joints, relatively planar breaks with little or no obvious displacement parallel to the plane; shears, structural breaks where very limited differential movement has occurred along a surface or zone of failure; and faults, sheared zones showing measurable offset with continuity which can be correlated between observation locations or are reported in the literature. The project area is mapped between two major strike-slip (generally near vertical with lateral motion) fault systems: the Straight Creek Fault Zone, approximately eight miles west of Newhalem, and the Ross Lake Fault Zone, approximately 12 miles east of Newhalem (Tabor *et al*., 2003). Additional faults mapped in the vicinity include the Triumph Fault (approximately five miles west of Newhalem) and the Thunder Lake Fault (approximately seven miles east of Newhalem). An anticline (convex-up fold) within the bedrock is mapped as trending northwest-southeast approximately through Newhalem (Brown and Dragovich, 2003). No major faults have been mapped in the project vicinity (Brown and Dragovich, 2003; Tabor *et al*., 2003).

3 Methodology

Collection of geotechnical data consisted of three components: data review, field exploration, and laboratory testing. Data review included collection and analysis of existing documents and information, including published geologic maps. The field exploration program included geologic reconnaissance and mapping, exploratory drilling, permeability (packer) testing, groundwater monitoring, and downhole optical televiewer imaging. Laboratory testing included unconfined compressive strength (UCS) testing, point load strength testing, and petrographic analysis of selected core samples to determine lithology and mineralogy. Methodology is explained in more detail in the following sections.

3.1 Data Review

3.1.1 Existing Data Review and Preliminary Geologic Assessment

An existing data review was conducted by Aspect and JA as part of a Preliminary Geologic Assessment, which was submitted to Seattle City Light on April 24, 2009 (Aspect and JA, 2009). This report included a literature and data review, a summary of known geologic conditions, and an existing geologic map of the project area. G1T tunnel records and inspection reports are included in Appendix A of the Preliminary Geologic Assessment. Existing geologic and geotechnical data and observations from throughout the G2T alignment vicinity are attached as Appendix I of this GDR. A summary of Appendix I data sources is included in Section 5.

3.1.2 LiDAR Lineament Analysis

Five oriented hillshade LiDAR (Light Detection and Ranging) images of the project area and surrounding vicinity were created and reviewed in order to identify lineaments (linear topographic features) of unknown origin, which may represent faults or other discontinuities within the bedrock. Generally, lineaments most frequently result from deposition and erosion of differing geologic materials, or jointing, faulting, or other tectonically-controlled phenomena. Aerial LiDAR survey data for the project area and extending along the Skagit River valley as far east as Ross Dam, approximately seven miles east of the Gorge Dam, was acquired by the U.S. Geological Survey in 2006. These LiDAR data were contracted by the U.S. Geological Survey and are available through the Puget Sound LiDAR Consortium (U.S. Geological Survey, 2006) as sets containing individual latitude, longitude, and elevation points (termed XYZ data) measured with one-meter (3.28-foot) or greater horizontal accuracy and 18.5-centimeter (7-inch) to 37-centimeter (15-inch) vertical accuracy on the ground surface. Point XYZ returns from the survey include tree top and vegetation canopy as well as the last return which is considered to be from the “bare earth”. A digital elevation model (DEM) of the ground surface was generated from these bare earth data, which was in turn used to generate topographic contour maps and light shaded (artificially illuminated) relief maps.

Lineament analysis was conducted in conjunction with field mapping using these detailed topographic maps. LiDAR map generation consisted of plotting the regional and site-specific area of interest using artificial illumination angles from four compass quadrants in addition to a set generated by combining light from the northwest, north, and northeast into a north composite projection. Lineaments were then plotted on individual maps. Some lineaments were apparent on a specific hillshade projection angle so

each quadrant hillshade map was analyzed separately and the lineaments from each were combined on the north composite image (Figure 3). Select LiDAR lineaments were then studied in the field, as detailed in Section 3.2.1. LiDAR hillshade images are included in Appendix H.

3.2 Field Exploration Program

Field exploration consisted of geologic reconnaissance, geologic mapping, exploratory geotechnical drilling, borehole permeability (packer) testing, groundwater monitoring, and oriented optical imaging of boreholes.

3.2.1 Geologic Reconnaissance and Mapping

A geologic reconnaissance was conducted on March 10, 2009, by JA and Aspect. Work consisted of selection of potential portal locations and exploratory borehole drill sites, as well as preliminary identification of major sets of joints and locations of possible faults.

Field mapping was conducted from April 20 to April 24, 2009, by JA and Aspect. Mapping consisted of measuring fault, joint, and foliation orientations using a Brunton compass, GPS, topographic maps, and shaded LiDAR elevation base maps. Potential faults and geologic structures, including those identified during LiDAR analysis (where accessible), were investigated, photographed, and measured. Lineaments that were confirmed to be faults, shear zones, or joints were directly observed to collect orientation, width, fracture density, infilling, weathering, and other data relevant to analysis of structures in the rock, with particular emphasis on structures that may be intercepted during tunneling and may have impacts on seepage and excavation stability. During the field mapping phase of the investigation, 46 joint orientation measurements and eight foliation orientation measurements were made throughout the alignment area, and 11 fault and fracture orientations were measured within the Devil's Elbow Adit (a horizontal construction access tunnel that extends from the Skagit River gorge to about the midpoint of the original Gorge tunnel and the approximate midpoint of the proposed G2T alignment; see Figure 2 for adit location) to characterize the rock mass. Measured structural data and dike and foliation orientations are presented in Appendix F.

3.2.2 Exploratory Borehole Drilling

Six boreholes were drilled between August 30 and October 14, 2009 in the vicinity of the proposed G2T alignment to characterize bedrock properties. Borehole locations are shown on Figure 2. Borehole depths ranged from approximately 360 to 800 feet, and were drilled at inclinations of 1° to 60° from horizontal. Angles of individual features noted on borehole logs and within core observations were measured from perpendicular to core axis and were not corrected to reflect the actual angle from horizontal. Unless otherwise noted, "depths" represent total length along the borehole and are not corrected for borehole inclination; they do not represent actual depths below ground surface. All "elevations" are corrected for borehole drill angle and therefore do represent actual projected elevations. Borehole methods, locations, and details are summarized in Table 1, and on individual borehole logs in Appendix A. Drill core photographs are presented in Appendix B.

All six boreholes were drilled by Crux Subsurface, Inc. (Crux), using the HQ wireline coring method. Total borehole diameter was 3.8 inches and total core diameter was 2.4 inches, according to drill bit specifications. Two Crux-built Burley drill rigs, Burley 5500-1 and Burley 5500-3, were used to drill all

six holes. Numerous diamond-impregnated drill bits of various hardnesses were used throughout the field exploration, including the Fordia Shark Advanced 13 and 15, Shark 13, and T Xtreme 11-14 bits, and the Boart-Longyear Alpha 10 bit. Drill bits quickly became polished and were frequently sharpened or switched. Core was generally drilled and retrieved in 5-foot sections (runs) with variations in run length as dictated by drilling conditions and the decisions of the driller. Individual core run lengths, drill times, and other drilling observations are included on borehole logs in Appendix A.

Boreholes were not generally cased. Exceptions were B-1, which was cased to a depth of 15.6 feet in order to prevent problems resulting from drilling through boulders and fractured rock shallow in the borehole, and B-6, which was cased to a depth of 49.5 feet in order to inhibit loss of drill water which was occurring through joints shallow in the borehole. Both B-1 and B-6 were cased with HWT casing, which has an outside diameter of 4.5 inches.

Helicopter mobilization was required to transport the drill rig and supplies to the locations of boreholes B-2, B-3, and B-4. Ventilation, air quality monitoring, special illumination and onsite safety teams and other safety measures were required for boreholes B-3 and B-4, which were located underground in the Devil's Elbow Adit. All personnel that entered the adit were required to have successfully completed a confined space entry training course.

After completion, boreholes B-1, B-4, and B-6 were sealed with a grout mixture of bentonite and cement and were abandoned. Vibrating wire pressure transducer piezometers (VWPs) were installed in boreholes B-2, B-3, and B-5, as described below in Groundwater Level Monitoring. Boreholes were surveyed by Seattle City Light following completion of the field exploration. Surveyed borehole locations are listed in Table 1.

3.2.3 In Situ Hydraulic Conductivity (Packer) Testing

In situ hydraulic conductivity, or packer, testing, is a type of permeability testing that can be conducted in boreholes of any inclination. Packer tests were performed in test sections where core logging and drill activity indicated a likelihood of high permeability. Targeted test sections included areas of heavily fractured rock and depths where a loss of drilling fluid circulation occurred or artesian groundwater conditions were encountered during drilling.

A total of eight packer tests were conducted in four of the boreholes. Desired test sections were isolated using either a single packer or straddle type packer. In the case of a straddle packer, the test section was sealed at either end of the pipe with inflatable packers, and water was injected through a 20-foot section of perforated pipe located between the packers. Where a single packer was used, the bottom of the borehole formed the bottom of the test section and a single packer sealed off the upper limit of the test section.

Packer test sections were tested using an injection method in which water was pumped into the test section at five-minute-long steps of constant pressure. The injection was generated with a 20-gallon per minute (gpm) pump located outside the borehole. Constant pressure was achieved by controlling the injection flow rate using a bypass valve. Pressure was measured using a 100 psi gauge and flow rate was measured using a totalizer and stopwatch. Pressure and rate of injection were recorded every minute.

Given sufficient data, packer tests can be used to calculate transmissivity (T), which can then be divided by the thickness of the saturated flow layer to determine hydraulic conductivity (K). Transmissivity is calculated by means of the Thiem equation (Thiem, 1906; and Driscoll, 1986), which is Darcy's law (the equation governing fluid flow through a saturated porous medium) applied to induced flow through a borehole.

Packer test data were analyzed for hydraulic conductivity following completion of the field exploration. In many cases, various factors rendered insufficient data to determine specific *K* and *T* values, however, packer tests did supply information regarding general hydraulic conductivity conditions and connectivity of fracture systems. Descriptions and results of individual packer tests are described in Section 4.6. Packer test data sets are presented in Appendix E. A summary of hydraulic conductivity conclusions is included as Table 4.

3.2.4 Groundwater Monitoring

Groundwater conditions were monitored through the collection of water level readings in three boreholes using Geokon vibrating wire pressure transducer piezometers (VWPs), and measurements of groundwater discharge rate and temperature where artesian flow occurred.

Artesian groundwater conditions were encountered in boreholes B-1 and B-3 during drilling and before abandonment. Groundwater discharge rate and temperature were measured in each of the two boreholes after or near drilling completion and before abandonment. Discharge from B-1 was measured 17 times over 43 days, and discharge from B-3 was measured five times over 10 days. Flow rates were observed by measuring the time taken to fill a 5-gallon bucket. The measurements possibly under-report the actual discharge due to groundwater that may have partially infiltrated into shallower densely fractured zones, and the bucket may not have caught all of the water discharging from the borehole during measurements. Temperatures of the discharge were measured using a hand held temperature probe. Artesian flow measurements are discussed in Section 4.5 and summarized in Table 3.

VWPs were installed for water level monitoring in boreholes B-2, B-3, and B-5. Each VWP was field-calibrated prior to installation. The VWPs were then taped to a ¾-inch PVC tremie pipe to ensure the proper depth was reached during installation. The tremie pipe was lowered down the hole until the VWP reached the desired depth and was then grouted in place through the tremie pipe from bottom to top using a mixture of bentonite and cement. The tremie pipe was abandoned in the hole with the VWP. VWPs were installed within approximately one foot of the maximum depth of each of the three boreholes (in some cases a small amount of blockage or slough prevented VWPs from reaching the total extent of the borehole). VWP depths were double-checked by tracking the total length of tremie pipe used.VWP installation details are summarized on Table 1 and on individual borehole logs in Appendix A.

Water levels were monitored using electronic dataloggers installed at the borehole surfaces. Dataloggers were programmed to record groundwater levels every 12 hours. Data were downloaded from the loggers on November 18, 2009, at which point fresh batteries were installed and the dataloggers were re-programmed to continue monitoring every 12 hours. Recorded VWP frequencies were then converted into groundwater elevations using factory-specified calibration factors unique to each VWP and standard formulas supplied by the manufacturer, and then plotted onto hydrographs. Groundwater elevation and temperature data are presented in Appendix D, along with the Geokon VWP manual and individual calibration sheets for each VWP.

Upon downloading data on November 18, 2009, it was discovered that the VWP installed in B-5 had not been recording data at the specified interval, apparently due to faulty batteries. Batteries were exchanged and the datalogger was re-programmed and appeared to be functioning properly; VWP readings taken on November 18, 2009, currently represent the only reliable water level readings from this borehole.

3.2.5 Oriented Borehole Imaging

Oriented downhole borehole imaging was conducted by Crux in order to help characterize bedrock, foliation, and fracture conditions. A Mount Sopris optical borehole probe was used to record high resolution imagery. An imbedded gyroscope allowed the unwrapped 360° recorded images to be directionally oriented, along with any joints or foliation apparent in the image. Crux identified planar features recorded by the images and used software to determine their orientations. A total of 1,016 feet of downhole imagery were recorded from boreholes B-1, B-2, B-3, B-5, and B-6. Borehole B-4 did not contain many joints of interest and was not imaged. Oriented borehole image data are presented in Appendix G.

3.3 Laboratory Testing

Geologic and geotechnical laboratory testing was performed on selected core samples obtained from the boreholes. Laboratory test procedures are described in the following sections. Laboratory test results and photos of samples submitted for unconfined compressive strength (UCS) testing, petrographic analysis, and point load testing results are included in Appendix C.

3.3.1 Unconfined Compressive Strength (UCS)

Unconfined compressive strength (UCS) testing is a method of determining the strength of intact rock core specimens. Rock core samples were selected from various depths in each borehole, with the goals of approximating the representative abundance of each rock type in the core, and of distributing the tests representatively throughout the boreholes and the proposed tunnel alignment length. A total of 29 samples were submitted to Hayre McElroy and Associates, LLC (Hayre McElroy), where testing was performed in general accordance with American Society of Testing and Materials (ASTM) method D7012.

Specimens of lengths greater than twice the core diameter were extracted and submitted to Hayre McElroy, where the core length was further trimmed until an approximate aspect ratio of length equal to twice the diameter was reached, and the ends were ground flat. Each specimen was then placed in a loading frame, where the axial load was continuously increased until the specimen failed. Peak load and failure type were recorded, and peak load was then divided by average cross sectional area into a uniaxial unconfined compressive strength value. UCS results are summarized in Table 6. A histogram of UCS results by rock type (for gneiss and migmatite) is included as Figure 10. Complete UCS test data are included in Appendix C.

3.3.2 Point Load Strength

The point load strength method is an index test used to estimate the compressive strength of hard rock specimens. Because the testing machine is highly portable and the method is rapid compared to the unconfined compressive strength method, point load testing is a relatively flexible and inexpensive way to augment rock strength data.

Diametral point load testing was conducted on 110 samples by Aspect between November 16 and November 23, 2009 using a portable Matest A125 point load tester, and was performed in general accordance with ASTM method D5731. Samples were selected in order to encompass a representative

number of each rock type encountered during the core drilling program. Ninety-five of the samples had preferred aspect ratios with lengths equal to or greater than diameter; fifteen of the samples analyzed had aspect ratios of length slightly less than diameter. The tests of samples with lengths less than diameter are technically not standard in ASTM methodology and are noted as such on the results, but were conducted in order to provide additional, potentially valuable data.

Each core sample was placed radially between two conical, truncated platens held in place by a loading frame. The core specimen was then subjected to an increasing load by use of a pneumatic hand pump, until failure was achieved. Peak failure pressure was recorded by a gauge and was transcribed along with observations regarding the rock core sample and failure type.

Twenty-one of the point load tests were conducted on samples also tested with the UCS method. Where possible, point load test results were compared to UCS results in order to establish a correlation factor (necessary in order to convert point load test results to equivalent UCS values) that could be applied to the remainder of point load test results. A best-fit, site-specific correlation factor of C=30.5 was determined from the data, which is approximately 125 percent of the standard correlation factor of C=24.5 (recommended by ASTM for the given core diameter- 60 mm or ~2.4 inches- when a site-specific correlation factor is unavailable).

The precision of the established site-specific correlation factor was questionable due to the wide scatter displayed by the UCS and point load values. The scatter was likely the result of a number of factors including variations in foliation angle, degree of foliation, foliation angle relative to platens (and relative to pressure direction for UCS tests, which is generally perpendicular to that of point load tests), and variability within rate increase from using the manually-controlled pneumatic pressure lever. It was determined that the standard ASTM correlation factor of 24.5 should be used to convert point load test data to UCS-equivalent data, and that more test points would be necessary in order to confidently select a site-specific correlation value within this foliated rock.

Point load test results are included as Appendix C.4. A histogram of point load test results by rock type (for gneiss and migmatite) is included as Figure 11.

3.3.3 Petrographic Analysis

Petrographic analysis was conducted in order to characterize mineral composition of each major rock type encountered during field exploration, and to identify secondary minerals not easily recognized in the field that could have an impact on tunnel design. Eleven specimens were selected from drill core samples and submitted to Spectrum Petrographics, Inc. (Spectrum) for thin section analysis.

Samples were analyzed and photographed in plane-polarized and cross-polarized light. Foliated specimens were ground down perpendicular to foliation where possible, in order to analyze the most representative sample possible. Results of thin section analysis include lithology, mineral percentage estimation, texture description, alteration, and method. The small size (27 x 46 mm) of thin sections analyzed did not accurately characterize pegmatite mineralogy and texture due to the large grain size of the pegmatite, which includes very coarse (<20 mm) crystals.

4 Subsurface Observations

4.1 Rock Types

Bedrock throughout the tunnel alignment area is composed primarily of biotite quartz plagioclase gneiss, some of which displays migmatitic and layered textures due to partial melting, and minor igneous intrusions. The root descriptive term “gneiss” was chosen rather than “schist” (which is used in petrographic results included in Appendix C) to describe metamorphic texture based on standard usage of the two terms, including a lack of platy fissility which is generally implied by the term schist, and lithologic descriptions based on previous field mapping in this area (Brown and Dragovich, 2003; Tabor *et al.*, 2003).

Four major rock types were identified during drilling explorations:

- Biotite Quartz Plagioclase Gneiss
- Migmatitic Biotite Quartz Plagioclase Gneiss
- Pegmatite
- Andesite

Detailed descriptions of each rock type are presented below. Histograms showing rock type distribution by borehole are included as Figures 4 through 9. A summary of petrographic results is displayed in Table 5. Complete results of petrographic analysis are included in Appendix C. For definitions of descriptive terms used in the following sections, see the Borehole Log Summary Key in Appendix A.

4.1.1 Biotite Quartz Plagioclase Gneiss

Biotite quartz plagioclase gneiss, mapped as orthogneiss by Tabor *et al*. (2003), was the most prevalent (approximately 79 percent of total core length drilled) rock type identified during field exploration. This rock type was encountered in all six boreholes. The gneiss is typically tonalitic (contains between 20 and 60 percent quartz) in composition, though it may contain zones of quartz dioritic (less than 20 percent quartz) composition. Mineral percentages estimated during petrographic analysis of thin sections made from six specimens indicate that primary minerals in the rock are plagioclase feldspar (30 to 55 percent), quartz (20 to 30 percent), and biotite (10 to 25 percent).

Secondary minerals of significant proportions include actinolite (0 to 20 percent), garnet (0 to 25 percent), sericite (15 percent in a highly altered sample), and hornblende (0 to 5 percent). Garnet was generally found in crystals ranging from <1/16-inch to (sparsely-found) ½-inch in diameter, but that were generally <1/8-inch in size. The hardness of garnet ranges from 6.5 to 7.5 on the Moh’s scale, whereas the hardness of quartz is 7. On an absolute scale, garnet can be up to 1.5 times as hard as quartz. Hornblende was identified only in field samples, and was not present in any of the petrographically analyzed samples. Additional accessory minerals are also present in lesser percentages, including clay minerals (0 to 1 percent), apatite (<1 to 2 percent), sphene (0 to 4 percent), chlorite (0 to 1 percent), leucoxene (0 to <1 percent), zircon (0 to <1 percent), “opaques” (<1 to 3 percent), and carbonate (0 to <1 percent). Opaques were classified by the petrographic laboratory as all minerals opaque to transmitted light. Chlorite is also locally pervasive within and near many healed joints, and in zones of alteration.

Field observations indicate the presence of trace amounts of pyrite in boreholes B-1, B-2, and B-3, both within the rock composition and on the surface of joints. At least some of the petrographically-identified

"opaques" are likely sulfides, indicating that the presence of sparse pyrite is likely in B-4, B-5, and B-6 as well.

Higher than typical percentages of leucoxene, dolomite, sericite, and other minerals, were found to be present locally in a highly altered sample from borehole B-3 (see Table 5 for details). Additional secondary or accessory minerals not identified during laboratory testing may also be present within this rock type.

Overall, the gneiss is generally medium to fine-grained, but includes medium to coarse-grained zones (see Borehole Log Summary Key in Appendix A for definitions). Color ranges from light to dark gray, or is white or gray with black. The fine-grained gneiss, though mineralogically similar to the medium-grained gneiss, often appears as a darker shade of gray. The gneiss unit is generally poorly to moderately foliated, but contains strongly foliated zones as well. Foliation orientation varies greatly throughout each borehole and within short distances of core.

Texture is generally gneissic but may include areas of schistose texture locally. Zones where migmatitic texture is dominant are described below in Section 4.1.2. Petrographic analysis indicates that portions of this rock may have experienced cataclastic metamorphism, or crushing and grinding. This was observed in one highly altered sample (extracted from B-3 at 281 feet) that was labeled a "cataclasite" in petrographic results. This zone was likely weakened and partially crushed during faulting, and left susceptible the flow of fluids that altered the matrix. The particular sample analyzed was highly altered, though partial cataclastic texture may be present in other faulted or disturbed zones that have not been visibly altered.

Thin quartz and/or feldspar-rich veins (generally less than 1 to 2-inches, but up to 12-inches) and andesite dikes, generally less than 1 to 2-inches, are scattered within this rock type. Veins, dikes, and mineralogically-distinct layers less than 12-inches-thick within this unit are also described as bands in borehole logs. Andesite dikes greater than 12-inches-thick were logged as a distinct rock unit. Rock is generally fresh to slightly weathered and includes local zones of moderately to highly weathered zones.

While variations in mineral content may result in a range of rock strength for this unit, rock is most commonly strong, but ranges generally from moderately strong to very strong. Local alteration and faulting may result in lower rock strengths that range to very weak or extremely weak within concentrated zones. Rock quality designation (RQD) is mostly excellent but ranges to very poor. Fracture density is primarily massive to slightly fractured. See Table 8 for complete fracture density percentages within this rock type. See Figures 10 through 13 for histograms of UCS and point load test rock type strengths, fracture density, and rock quality designation (RQD) for biotite quartz plagioclase gneiss and migmatitic biotite quartz plagioclase gneiss.

4.1.2 Migmatitic Biotite Quartz Plagioclase Gneiss

Migmatites are highly metamorphosed rocks that were partially melted and therefore display a mix of igneous and metamorphic characteristics. Migmatitic biotite quartz plagioclase gneiss with tonalitic composition was the second-most prevalent rock type (approximately 18 percent of total core length drilled) encountered during subsurface exploration. This rock type was encountered in all six boreholes. The migmatite consists generally of irregularly intermixed and marbled layers of dark-colored (biotite-rich) layers, light-colored (quartz and feldspar-rich) layers, and biotite quartz plagioclase gneiss layers.

Petrographic results of two migmatitic specimens indicate a slightly higher quartz content (32 to 39 percent) and slightly lower biotite content (13 to 15 percent) than the biotite quartz plagioclase gneiss. However, the texture of migmatitic sections varied greatly between boreholes, and strong banding and mineral segregation complicates estimation of overall mineral percentages within the unit. Migmatitic

texture varies greatly, from displaying distinct, well foliated near-parallel bands (mineralogically segregated layers) to highly deformed, marbled, swirled, and folded layers with cross-cutting veins and dikes.

Mineral content, estimated from field observations and three laboratory petrographic analyses, is similar to that of biotite quartz plagioclase gneiss (see Section 4.1.1), though higher percentages of some minerals may be observed in migmatite thin sections due to the size of mineralogically-segregated bands relative to the sample size. Primary minerals in the rock are plagioclase feldspar, quartz, and biotite. Overall, the migmatitic gneiss is generally medium to fine-grained, but includes medium to coarse-grained zones.

Strength of this rock type is generally strong to moderately strong, but ranges to weak. Local alteration and faulting may result in lower rock strengths that range to very weak or extremely weak within concentrated zones. Rock quality designation (RQD) is mostly excellent but ranges to very poor. Fracture density is primarily massive. See Table 8 for complete fracture density percentages within this rock type. See Figures 10 through 13 for histograms of UCS and point load test rock type strengths, fracture density, and rock quality designation (RQD) for biotite quartz plagioclase gneiss and migmatitic biotite quartz plagioclase gneiss.

4.1.3 Pegmatite

Pegmatites are intrusive igneous rocks containing very coarse (<20-mm or <0.8-inch) crystals. Pegmatites along the G2T alignment generally consist of white to light gray quartz and feldspar-rich rock that cut through the gneiss bedrock in concordant and discordant veins and dikes. Pegmatite dikes make up only approximately two percent of total core length drilled. Pegmatite was observed in boreholes B-1 (four percent of borehole core length), B-2 (one percent of borehole core length) B-3 (one percent of borehole core length), B-4 (five percent of borehole core length) and B-5 (two percent of borehole core length).

Mineral composition generally consists of approximately 50 percent plagioclase feldspar, 40 percent quartz, and 10 percent biotite. However, localized portions of pegmatite may contain up to 30 percent biotite. Trace (up to one percent) secondary minerals identified in petrographic analysis were clay, apatite, and chlorite, though additional secondary minerals could be present in other locations. Garnet was not commonly observed during field explorations, and was generally less than one percent where present. Pegmatite intrusions typically range up to approximately five feet thick, though could potentially thicker dikes could be encountered.

Grain size within the pegmatite generally ranges from coarse to very coarse-grained. In some locations, pegmatites contain fine and medium grains where partial cataclastic metamorphism has occurred, meaning that the rocks have experienced crushing or grinding and mineral grains have since been re-healed. This texture is indicated in petrographic results by the term “cataclasite.” The partial crushing and grinding likely occurred during emplacement of the pegmatite dike as it intruded into the surrounding country rock. Only one pegmatite sample was submitted for petrographic analysis, and it is likely that the sample may have over-represented the cataclastic texture and under-represented the pegmatitic texture of the overall rock type due to the small sample size available for analysis.

Pegmatite is generally moderately strong to strong, with local weak zones. This rock type was generally observed to be fresh or slightly weathered. Rock quality designation (RQD) is mostly excellent (90 percent), and ranges to fair (ten percent of total). This rock type is primarily massive. See Table 8 for complete fracture density percentages within this rock type.

4.1.4 Andesite

Intrusive porphyritic andesite dikes less than 1-foot-thick were found in minor quantities cutting through other rock types throughout the alignment area. Andesite dikes greater than one foot make up only approximately one percent of overall core length drilled. Andesite dikes were observed in boreholes B-2 (three percent of borehole core length), B-5 (one percent of borehole core length) and B-6 (three percent of borehole core length).

The sample of andesite tested for petrographic analysis was composed of approximately 65 percent plagioclase feldspar, 20 percent biotite, and 10 percent hornblende. Secondary minerals include quartz (2 percent), sphene (1 percent), and opaques (2 percent). No garnet was observed in this rock type during the field exploration.

Andesite intrusions were generally observed to be porphyritic in texture, consisting of an aphanitic (crystals too small to see) groundmass with embedded visible, fine-grained phenocrysts. In most locations, andesite forms gray to black, thin, fine-grained cross-cutting dikes, generally ½-inch to six inches in thickness. Andesitic dikes from one- to three-feet-wide were observed in boreholes B-5 and B-6, and a 20-foot-thick dike was present in borehole B-2. Andesite intrusions are greenish gray where chlorite is present as an alteration product. Contacts between andesite intrusions and surrounding rock are often diffuse.

Andesite is generally strong, but ranges from very weak to very strong. This rock type was commonly observed to be fresh or slightly weathered. Rock quality designation (RQD) is mostly excellent (63 percent), and ranges to poor (13 percent of total). The remaining rock is 13 percent fair and 13 percent good. This rock type is primarily highly fractured (32 percent of total rock type) or moderately fractured (29 percent). See Table 8 for complete fracture density percentages within this rock type.

4.2 Fractures

Fracture density within bedrock throughout the G2T alignment vicinity is primarily massive to slightly fractured, though all boreholes also contained sections of moderately, highly, and intensely fractured rock. Boreholes B-2, B-3, and B-4 consisted of primarily massive rock, and boreholes B-1, B-5, and B-6 consisted of primarily slightly fractured rock. Percentages of massive rock and of and slightly, moderately, highly, and intensely fractured rock are displayed by borehole in Table 7. All rock types were primarily massive except for andesite, which was primarily highly fractured and slightly fractured. Percentages of fracturing by rock type are shown in Table 8. Fractures are illustrated in the fracture sketch column on individual borehole logs in Appendix A, and are described in the discontinuity description column of borehole logs.

All boreholes contained evidence of at least minor shears or fault zones. Possible faults were identified in boreholes B-2 at approximately 199 feet, B-3 at approximately 293 feet, and B-5 at approximately 95 feet. Significant intensely fractured zones include those in B-1 from approximately 235 to 246 feet and 257 to 265 feet, B-2 from approximately 67 to 73 feet, B-5 from approximately 94 to 103 feet, 122 to 138, feet and 361 to 370 feet, and B-6 from approximately 34 to 46 feet. For complete description and illustration of fracture and possible fault zones, see borehole logs in Appendix A.

4.3 Surficial Deposits

Surficial deposits were encountered in B-1 and B-6. These deposits primarily include boulders that have been moved downslope by gravity-influenced processes or weathered in place out of near-surface bedrock, as well as alluvial sediments deposited by water which include gravel, silty sand, and gravelly sand. Surficial deposits are described in more detail in the borehole logs (Appendix A) in which they were encountered.

4.4 Drilling Conditions

Drilling conditions were variable throughout the boreholes due to drill equipment, driller, weather and topography, bit type, rock type, rock quality, mineral assemblage, water conditions, and other factors. The total duration of the field program was extended and the total drill footage was decreased from projected estimates due to slower-than-expected drilling. A total of 2787.6 feet were drilled over 79 drill days. Drillers indicated higher-than-expected bit polish throughout the duration of fieldwork, and frequently switched out drill bits or attempted to roughen the bits to expose new diamonds. A hard bit with a wide range such as the Fordia T Xtreme 11-14 seemed to be the drillers' preferred choice in order to make good progress while not overly-polishing the bit. The Fordia Shark Advanced 13 was also commonly used toward the end of the drilling program. The average drilling rate was approximately 35 feet per 10-hour day. Total drill days per borehole and daily average drilling rates per borehole can be found in Table 1.

4.5 Groundwater Observations

Groundwater was observed in three boreholes (B-1, B-2, and B-3) during drilling, as well as prior to grouting. The maximum depth to water measured in the inclined B-2 borehole during drilling was 300 feet (approximate 260 feet vertically below ground surface), while artesian conditions were encountered in B-1 and B-3. At-time-of-drilling (ATD) water level observations are presented in Table 2 and on individual borehole logs in Appendix A. A detailed summary of discharge flow rates and temperatures for boreholes B-1 and B-3 are presented in Table 3, and are summarized below.

Artestian flow was first measured in borehole B-1 during drilling at a rate of approximately 0.75 gpm at a drill depth of 260 feet, after the borehole had been left open overnight. Artesian flow increased to about 10 gpm by drill depth 320 feet, 20 gpm by 325 feet, and 55 gpm by 325 feet. After reaching the total drill depth of 360.8 feet, rate of discharge was estimated at 30 gpm. In the approximately five weeks that followed, B-1 artesian flow was measured at between approximately 19 and 31 gpm over 12 measurement days. Discharge water temperature for B-1 was measured at between 8.2 and 8.6 degrees C over three measurement days.

Artesian flow was first measured in borehole B-3 during drilling at rate of approximately 2.6 gpm at a drill depth of 360 feet. After reaching the total drill depth of 399.2 feet, rate of discharge was estimated at 3 gpm. In the nearly two weeks that followed, B-3 artesian flow was measured at approximately 3 gpm over three additional measurement days. Discharge water temperature for B-3 was measured at between 11.7 and 12.4 degrees C over two measurement days.

Automatic datalogger readings indicate that maximum water level elevations between the time of installation and download on November 18, 2009, were 855 feet in B-2 and 780 feet in B-3. A sharp decline in water level of about 47 feet in B-2 beginning after October 27, 2009 resulted in a minimum

water level elevation of 808 feet on November 4, 2009. This event likely correlates with a drawdown of 22 feet in Gorge Reservoir level which occurred on October 28, 2009. The minimum water level elevation for B-3, recorded on October 3, 2009, was 740 feet. The sole reading from the B-5 VWP resulted in a water level elevation of between 794 feet. Time series of water level elevations and water temperatures in the three boreholes can be found in Appendix D.

4.6 In Situ Hydraulic Conductivity (Packer) Testing Results

Testing in B-2 at the 285 to 305-foot depth interval indicates a hydraulic conductivity (*K*) value of $2x10^{-6}$ centimeters/second (cm/s). Other packer test results did not yield *K* values when traditional methods of analysis were applied, however, test results as described below do provide general information regarding hydraulic head, response to injected flow, and relative hydraulic conductivity or connectivity of fracture systems.

Due to flowing artesian conditions during packer testing in B-3 at the 356 to 376-foot depth interval, hydraulic conductivity cannot be quantified using standard methods. However, by assuming the hydraulic gradient is equal to the difference in head applied during testing and the top of borehole elevation, a value may be estimated. Using this assumption, we calculate a minimum hydraulic conductivity value of approximately $4x10^{-3}$ cm/s.

Pressures observed during testing did not exceed the baseline value for friction loss through the small diameter injection line at the maximum flow rate for packer tests in B-5 at the 305.7 to 325.7-foot depth interval and in B-6 at the 244.3 to 273.3 and 279.3 to 299.3-foot depth intervals. Hydraulic conductivity values are greater than the supply capacity of the testing equipment needed to quantify the conductivity. However, by assuming the injected flow rate was accepted by the full 20-foot test interval under unit gradient conditions, we estimate minimum *K* values of approximately $1x10^{-1}$ cm/s for the specified depth intervals (Table 4).

Due to the near-vertical borehole and the static depth to water, hydraulic conductivity in B-2 at the 701 to 800-foot depth interval was greater than the supply capacity of the testing equipment. This interval took 20 gpm of water for a duration of 15 minutes with no response in the gauge pressure at the ground surface.

Analysis of B-3 at the 270 to 290-foot depth interval indicates that the fracture system within this interval is tight, and that hydraulic conductivity is relatively low. A minimum *K* value of 4×10^{-3} cm/s was calculated for this interval using data not including the final pressure step-down to 10 gpm where backflow conditions occurred. Testing in B-5 at the 221.7 to 245.7 foot depth interval was similarly non-quantifiable with traditional methods because the hydraulic conductivity of the testing intervals was too low to accept measurable quantities of water. However, the minimum hydraulic conductivity of this interval is assumed to be greater than the lower limit of testing, calculated at approximately $K = 4x10^{-6}$ cm/s.

5 Reference Data Sources

Previously existing geologic and geotechnical data was compiled for our Preliminary Geologic Assessment (Aspect, 2009). A detailed summary of geological and geotechnical information relevant to G2T construction can be found in that report.

Reference data included in Appendix I of this GDR consists of previously conducted laboratory strength tests and petrographic analysis conducted by Hatch Mott MacDonald from 1997 (Appendix I.1), , a geologic report from Gorge High Dam construction with exploration logs (incomplete) from 1954 (Appendix I.2), a geologic examination of the Gorge High Dam Site from 1954 (Appendix I.3), Gorge Plant Extension plans, maps, borehole logs, and core photographs from 1945 to 1948 (I.4), and miscellaneous core logs and cross sections from the original Gorge power station and G1T construction from 1918 to 1923 (Appendix I.5).

It should be noted that the Hatch Mott MacDonald petrographic and strength tests were performed on samples of boulders taken from in the G2T alignment vicinity, including from the portal and intake areas. Test results conducted on boulders may differ from those conducted on bedrock in that boulders have been weathered and transported from an unknown source.

An additional note regarding the Gorge High Dam geologic report from 1954 is that regional and global geologic understanding has greatly advanced since that time, and data and interpretation within the borehole logs and text may be inconsistent with geologic data in this report. However, boreholes described in the 1954 report were not located along the G2T alignment, and some discrepancies between the two data sets may represent actual spatial variation in geologic characteristics.

6 References

Aspect Consulting, LLC, and Jacobs Associates, 2009. Gorge 2nd Tunnel Preliminary Geologic Assessment, Seattle City Light, April 24, 2009.

ASTM Standard D7012, 2004. "Compressive Strength and Elastic Moduli of Intact Rock Core Specimens under Varying States of Stress and Temperatures," ASTM International, West Conshohocken, PA, *www.astm.org.*

ASTM Standard D5731, 2002 (2005). "Determination of the Point Load Strength Index of Rock," ASTM International, West Conshohocken, PA, *www.astm.org*.

Brown, E.H., and Dragovich, J.D., 2003, Tectonic Elements and Evolution of Northwest Washington, Washington Division of Geology and Earth Resources map GM 52.

Driscoll, Fletcher G., 1986, Groundwater and Wells, Second Edition. Johnson Division, St. Paul Minnesota, p. 212-213.

Hatch Mott MacDonald, 2007, Gorge Powerhouse Companion Tunnel: Conceptual Cost Estimate Study (Appendix A), Seattle City Light, February 2007.

Royle, Michael, 2009. Standard Operating Procedures for Borehole Packer Testing. SRK Consulting, Vancouver, British Columbia. Available at: *http://www.robertsongeoconsultants.com/admin/upload/Packer_testing.pdf*

Thiem, G., 1906. Hydrologische Methoden. Leipaig, 56 p.

Tabor, R.W., Haugerud, R.A., Hildreth, W., and Brown, E.H., 2003, Geologic Map of the Mount Baker 30- by 60-Minute Quadrangle, Washington, U.S. Geologic Survey. Geologic Investigations Series I-2660.

U. S. Geological Survey, 2006, 2006 USGS North Puget Sound LIDAR Survey; available through the Puget LIDAR Consortium, (http://pugetsoundlidar.ess.washington.edu/lidardata/restricted/usgs2006nps/)

7 Limitations

Work for this project was performed, and this report prepared, in accordance with generally accepted professional practices for the nature and conditions of work completed in the same or similar localities, at the time the work was performed. It is intended for the exclusive use of Seattle City Light for specific application to the referenced property. This report does not represent a legal opinion. No other warranty, expressed or implied, is made.